

## Phase III: Final Report



Figure 1: Cooler Master Hyper TX-3

### Executive Summary

Our task was to, given a CPU heat sink, research its operational performance requirements, then model and conduct simulations and tests to determine whether the heat sink will be able to meet the performance requirements. Our heat sink must be able to maintain a heat flux of 140W while keeping the base surface temperature under 64°C. Based on our simulations and a real-world test, our heat sink can perform this task easily. Additionally, our simulations found that the heat sink can maintain the base surface temperature below 64°C with a heat flux of up to 165W with the measured velocity of 0.58 m/s and up to 288W with the max manufacturer specified fan velocity of 3.86 m/s. Lastly, we simulated the effects of possible improvements to the system. Lastly, we simulated the effects of possible improvements to the system with respect to both cost and thermal performance. For cost, we suggested removing the fan and reducing fin thickness (to 57% of the original), which yielded temperatures of around 300 C and 47°C respectively. For thermal performance, we suggested changing the fin material to copper and doubling fan speed, which both produced temperatures near 39.5°C. Analysis of the simulation results concluded that forced convection is essential to the system, but fin thickness can be shortened to reduce cost. Also, changing the fin material to copper and doubling the fan speed yields slightly better thermal performance.

## Investigation Framework

The diagram in Figure 2 shows a brief summary of the investigation framework. Here we lay out the details:

1. Hand Calculations (Do this for both measured velocity and manufacturer specified velocity)
  - a. Find the fin efficiency to determine if rectangular fin analysis is sufficient.
  - b. Find the Reynolds number to determine if the flow is turbulent or laminar.
  - c. Compare the boundary layer to gap between two plates to determine if the flow is internal or external.
  - d. For turbulent flow, find reciprocal of Graetz number to determine if the flow is fully developed.
  - e. Use the corresponding Nusselt correlation to calculate convection coefficient.
  - f. Account for radiation and check the significance of free convection.
  - g. Calculate the heat sink base temperature.
2. SolidWorks Simulations
  - a. Flow analysis
  - b. Element convergence test
  - c. Full and half model analysis
3. System Improvements
  - a. Brainstorm realistic ideas
  - b. Modify system on SolidWorks to match ideas and run simulation
  - c. Analyze results
  - d. Make conclusions

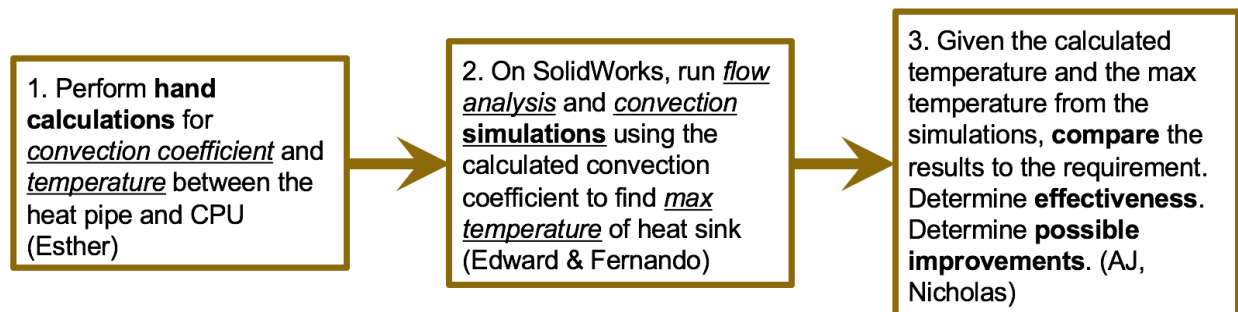


Figure 2: Investigation framework diagram

## Operational Parameters and Required Performance

The Cooler Master Hyper TX3 was released in early 2009 (Fig. 1). This puts the cooler in the era of Intel sockets LGA1156, 1155 and 775, as well as AMD sockets AM2, AM2+, and 939. Due to compatibility with socket mountings, the cooler is also compatible with the newer LGA1150 and AM3 sockets, as they share mounting compatibility with the older sockets. This means the cooler is compatible with a wide range of CPU's, from Intel's Pentium, Celeron, Core 2, Core i3, Core i5, to AMD's Athlon, Phenom, and FX series. Interestingly, Cooler Master specifies a maximum supported TDP of "over 130W" on the cooler specifications, which would include several processors in the Core i7 series, even though Cooler master does not explicitly list them.<sup>1</sup> More relevant is the AMD processors listed. Table 1 is a table of several of the most powerful CPUs from this time period that mount in compatible sockets, with their TDP and maximum temperature. Other, less powerful CPUs, as well as CPUs that do not use a socket this cooler is compatible with are not listed.

Table 1: Selected CPU's and their thermal properties

CPU	TDP (W)	Max Temp (°C)
Core i7 860 <sup>[4]</sup>	95	72.7
Core i7 2600K <sup>[7]</sup>	95	72.6
Phenom X4 9950 BE <sup>[1]</sup>	140	64
Phenom II X4 965 BE <sup>[1]</sup>	125	62

As shown by this table, and supported by our research, the hottest CPU is the AMD Phenom X4 9950 Black Edition, with a 140W Thermal Design Power, and a maximum temperature of 64°C, it is the most demanding CPU benchmark available. If the heatsink can keep this CPU within specifications, it can keep all of the others properly cooled as well. Thus, our final parameters are presented in Table 2.

Table 2: Required Performance Specifications

CPU	TDP (W)	Max Temp (°C)
Phenom X4 9950 BE	140W	64

## Detailed Analysis

### Fin Analysis

Table 3: Parameter Values

$T_{\infty}$ (°C)	$V_{measured}$ (m/s)	$V_{fan}$ (m/s)	$Q$ ( $m^2/s$ )
22	0.58	3.86	0.0256

Note: The ambient temperature, fan velocity, and airflow rate are based on test bench condition

Table 4: Properties of Air, Aluminum, and Copper

$k_{co}$ (W/mK)	$k_{Al}$ (W/mK)	$k_{air}$ (W/mK)	$\nu$ ( $m^2/s$ )	$Pr$
$10\sim 100\times 10^3$	170	$25.9\times 10^{-3}$	$15.43\times 10^{-6}$	0.708

### Goal

Given the maximum thermal power of the heat sink, find the temperature of the heat pipe at the contact point with the CPU.

### Assumptions

- Steady state conditions
- One dimensional radial condition in fins
- Constant properties
- Uniform convection coefficient over outer surface of fin
- Uniform surface temperature for copper heat pipe, which has high thermal conductivity
- No heat transfer between the aluminum base and the processor
- Negligible heat loss through convection or radiation for the heat pipes
- The plates are smooth

#### 1. Reynolds Number

$$Re_D = \frac{u_m D_h}{\nu} \quad (1)$$

We calculate the Reynolds number using Equation 1 for flow between parallel plates, where  $u_m$  is the mean velocity of the air flow,  $\nu$  is the viscosity of air, and  $D_h$  is the hydraulic diameter defined by:

$$D_h = \frac{4A_c}{P} = 2b \quad (2)$$

where  $A_c$  is the cross-sectional area between the plates,  $P$  is the wetted perimeter, and  $b = 0.00225$  m is the gap between two plates. Plugging in the parameter values and with  $V_{measured}$ ,

we get  $D_h = 0.0045 \text{ m}$  and  $Re_D = 169 < 2300$ . If we ignore the effect of fan movement, we can say that the flow is laminar.

Due to the motion of the fan, however, the flow is likely to be turbulent. Hence, we will do calculations for both laminar and turbulent cases, where we use  $Re_D = 2300$  for turbulence.

## 2. Radiation

Assuming copper heat pipe has negligible radiation, we model two adjacent fin plates as two parallel plates (Fig. 3a). From Table 13.2 in the textbook, we get a view factor of  $F_{12} = F_{21} = 0.93$ , where 1 and 2 correspond to each of the plates. We model the plates and the gaps between the plates separately. All of the gaps are combined and modeled as a big shell (Fig. 4b). All of the plates are combined and modeled as a big block of rectangular prism with no gaps (Fig. 4a). Each of the six surfaces of the prism don't see each other. Hence, we consider it as six cases of radiation between a wall and the surrounding, where the wall corresponds to each surface (Fig. 3b). For further simplification, we consider only three cases since there are three different surface areas of the prism, and later we will double our values to account for the other three.

The radiation exchange between two surfaces is defined by:

$$q_{ij} = A_i F_{ij} \sigma (T_b^4 - T_\infty^4) \quad (3)$$

where  $A_i$  is the surface area of surface  $i$ ,  $F_{ij}$  is the fraction of the radiation leaving surface  $i$  that is intercepted by surface  $j$ , and  $\sigma = 5.67 \times 10^{-8} \text{ W/m}^2 \text{K}^4$  is the Stefan-Boltzmann constant. Let 3, 4, and 5 correspond to three surfaces of different surface areas and 6 correspond to the surrounding. Then,  $F_{36} = F_{46} = F_{56} = 1$  and  $A_3 = 0.0042 \text{ m}^2$ ,  $A_4 = 0.0013 \text{ m}^2$ , and  $A_5 = 0.00069 \text{ m}^2$ . We also have to take into account the radiation leaving through the gaps between plates, which is  $q_{rad,gap} = n(1 - F_{12})q_{36}$ , where  $n = 82$  is the number of plate surfaces forming the gaps.

So the total radiation from the heat sink is calculated by the following:

$$\begin{aligned} q_{rad,total} &= 2(q_{36} + q_{46} + q_{56}) + q_{rad,gap} \\ &= 2\sigma(T_b^4 - T_\infty^4) \left\{ \left[ 1 + \frac{n}{2}(1 - F_{12}) \right] A_3 F_{36} + A_4 F_{46} + A_5 F_{56} \right\} \end{aligned} \quad (4)$$

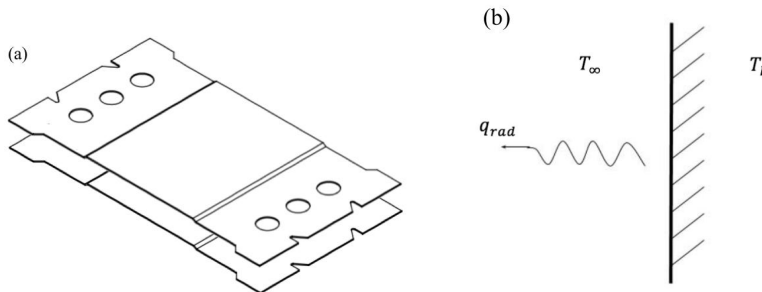


Figure 3: (a) Parallel-plate model, (b) radiation from wall

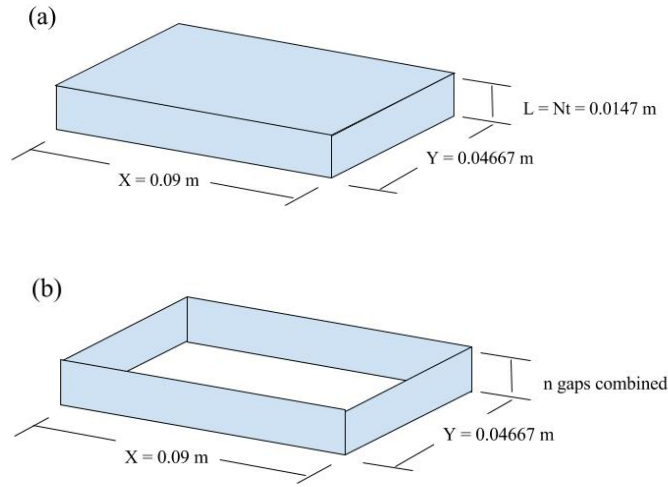
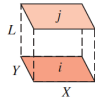


Figure 4: (a) Rectangular prism model for fins, (b) shell model for gaps

TABLE 13.2 View Factors for Three-Dimensional Geometries [4]

Geometry	Relation
Aligned Parallel Rectangles (Figure 13.4)	$\bar{X} = X/L, \bar{Y} = Y/L$ $F_{ij} = \frac{2}{\pi \bar{X} \bar{Y}} \left\{ \ln \left[ \frac{(1 + \bar{X}^2)(1 + \bar{Y}^2)}{1 + \bar{X}^2 + \bar{Y}^2} \right]^{1/2} + \bar{X}(1 + \bar{Y}^2)^{1/2} \tan^{-1} \frac{\bar{X}}{(1 + \bar{Y}^2)^{1/2}} + \bar{Y}(1 + \bar{X}^2)^{1/2} \tan^{-1} \frac{\bar{Y}}{(1 + \bar{X}^2)^{1/2}} - \bar{X} \tan^{-1} \bar{X} - \bar{Y} \tan^{-1} \bar{Y} \right\}$



## A. Turbulent Flow

### A.1 Boundary Layer

First, we calculate the velocity and thermal boundary layer thicknesses,  $\delta_v$  and  $\delta_t$ , of the turbulent flow using Equation 5 and 6 (Equation 7.35 and 7.24 from the textbook):

$$\delta_v = \frac{0.37x}{Re_x^{1/5}} \quad (5)$$

$$\delta_t = \frac{\delta_v}{Pr^{1/3}} \quad (6)$$

where  $Re_x = \frac{u_m x}{\nu}$ . To determine which length to use for  $x$ , we calculate the hydrodynamic entry length,  $x_{f,d,h}$ , and the thermal entry length,  $x_{f,d,t}$ , for turbulent flow, which are obtained from the following equations (Equation 8.4 from the textbook):

$$x_{fd,h} \approx x_{fd,t} \approx 10D_h \quad (7)$$

Plugging in the parameter values, we get  $x_{fd,h} \approx x_{fd,t} \approx 0.045 \text{ m}$ . Since  $x_{fd,h} < L = 0.04667 \text{ m}$ , the full length of the plate over which the air flows, we use  $x_{fd,h}$  for  $x$ . With this hydrodynamic entry length, we get  $Re_x \approx 1692$  and  $\delta_v = 0.0039 \text{ m}$  and  $\delta_t = 0.0043 \text{ m}$ . Both the velocity and thermal boundary layer thickness is greater than half the gap between the plates,  $\delta > b/2$ , which means the boundary layers of the two adjacent plates will overlap. Therefore, it is reasonable to treat the flow as internal.

Table 5: Entry lengths and boundary layer thicknesses for turbulent flow

$x_{fd,h} \text{ (m)}$	$x_{fd,t} \text{ (m)}$	$\delta_v \text{ (m)}$	$\delta_t \text{ (m)}$
0.045	0.045	0.0039	0.0043

## A.2 Heat Transfer Coefficient

Since the flow is internal, we can ignore free convection and only consider forced convection. The flow is turbulent and fully developed ( $L > x_{fd,h} \approx x_{fd,t}$ ), so we use the following correlation for Nusselt number (Equation 8.60 from the textbook):

$$Nu_D = 0.023Re_D^{4/5}Pr^{0.3} \quad (8)$$

from which we get  $Nu_D = 10.14$ . Then, we use Equation 9 to calculate the heat transfer convection coefficient of the forced convection:

$$h = \frac{Nu_D k_{air}}{D_h} \quad (9)$$

where  $k_{air}$  is the thermal conductivity of air. We get  $h = 58.4 \text{ W/m}^2\text{K}$ .

## A.3 Base Temperature

We make an assumption that the finned and prime surfaces have equal convection coefficient. Then, the total heat transfer rate due to convection from the surface area of the total  $N=42$  number of fins and the exposed portion of the base is defined as:

$$q_{conv} = hA_t \left[ 1 - \frac{NA_f}{A_t} (1 - \eta_f) \right] \theta_b \quad (10)$$

where  $\theta_b = T_b - T_\infty$  is the difference between the base temperature,  $T_b$ , and the surrounding temperature,  $T_\infty$ .

For the purpose of the analysis, we assume the plate is a perfect rectangle and divide the fin plate into two half-sections since it is symmetrical (Fig. 5a). We further divide the half section into two parts along the pipe holes so that we have a short fin on one side and longer fin on the other (Fig. 5b and 5c). We will do separate analysis for the short and long fins.

#### A.4.a Short Fin

The total surface area of the exposed portion of the short fins and the base is  $A_t = NA_f = 0.0415 \text{ m}^2$ , where  $A_f = 2(wL_2 - \frac{3}{2}\pi R^2) = 0.001 \text{ m}^2$ . Let  $L_c = L_2 + t/2 = 0.0117 \text{ m}$ . Then, the fin efficiency is obtained from the following:

$$\eta_f = \frac{\tanh(mL_c)}{mL_c} \quad (11)$$

where  $m$  is defined as:

$$m = \sqrt{\frac{4P}{k_{Al}A_c}} \quad (12)$$

The thermal conductivity of the aluminum fin is  $k_{Al} = 170 \text{ W/m} \cdot \text{K}$ . The perimeter of the fin is  $P = 2(w + t) = 0.094 \text{ m}$  and the cross-sectional area is  $A_c = wt = 1.63 \times 10^{-5} \text{ m}^2$ . Plugging in these values, we get  $m = 12.83 \text{ m}^{-1}$  and  $\eta_f = 0.99$ . Since the fin efficiency is close to one, we can assume that the temperature is nearly uniform along the heat pipe holes. Therefore, rectangular fin analysis is sufficient.

According to the specification of the commercial heat sink, the maximum heat transfer from the fin is  $q_{max} = 140 \text{ W}$ , which is combined radiation and convection. So the heat transfer only due to convection would be  $q_{conv} = q_{max} - q_{rad,total}$ . In actual calculation, we use only a proportion of  $q_{conv}$ , equivalent to the percentage of the area of the short fin over the total fin plate area.

Solving for the temperature of the base from Equation 10, we have:

$$T_b = \frac{q_{conv}}{hA_t \left[ 1 - \frac{NA_f}{A_t} (1 - \eta_f) \right]} + T_\infty \quad (13)$$

Using a numerical solver (Matlab, fzero) with all the given values, we get  $T_b = 29.4 \text{ }^\circ\text{C}$ .

#### A.4.a Long Fin

We perform similar analysis for the long fin, except  $A_f = 2wL_1 - \frac{3}{2}\pi R^2 = 0.003 \text{ m}^2$  and  $L_c = L_1 + t/2 = 0.0337 \text{ m}$ . We get the same  $m$  as the short fin and  $\eta_f = 0.94$ . Since the fin



efficiency of the long fin is also close to one, rectangular fin analysis is sufficient. Finally, from Equation 13, we get  $T_b = 29.3 \text{ }^\circ\text{C}$ .

If we use calculated Reynolds number for the case of turbulence, we get  $Nu_D = 1.26$ ,  $h = 7.23 \text{ W/m}^2\text{K}$ , and  $T_b = 75.5 \text{ }^\circ\text{C}$  for both short and long fins.

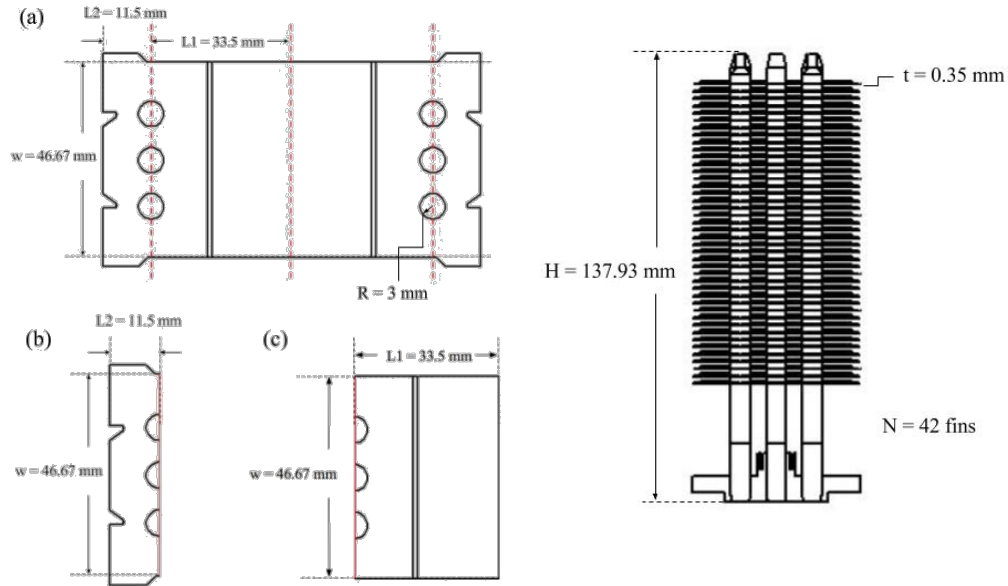


Figure 5: Fin plate divisions and dimensions

### A.5 Free Convection

To determine whether or not free convection is negligible, we calculate the following ratio:

$$\frac{Gr}{Re_D^2} \quad (14)$$

The Grashof number  $Gr$  was obtained from Equation 15:

$$Gr = \frac{g\beta(T_b - T_\infty)D_h^3}{\nu^2} \quad (15)$$

where  $T_b$  is the base temperature,  $T_\infty$  is the ambient temperature,  $g = 9.81 \text{ m/s}^2$  is the gravitational acceleration and  $\beta$  is the coefficient of thermal expansion,

$$\beta = \frac{1}{T_{avg}} \quad (16)$$

where  $T_{avg} = (T_b + T_\infty)/2$ .

Plugging in the numbers, we get  $\frac{Gr}{Re_D^2} = 1.75 \times 10^{-5} \ll 0.1$  for the short fin and  $\frac{Gr}{Re_D^2} = 1.74 \times 10^{-5} \ll 0.1$  for the long fin. Therefore, we conclude that our assumption that free convection is negligible is correct.

## B. Laminar Flow Analysis

### B.1 Boundary Layer

For laminar flow, we use the calculated  $Re_D = 169$ . The velocity boundary layer thickness,  $\delta_v$ , is obtained from Equation 17 (Equation 7.19 from the textbook):

$$\delta_v = \frac{5x}{\sqrt{Re_x}} = 0.005 \text{ m} \quad (17)$$

where  $Re_x = \frac{u_m x}{\nu}$  and to determine which length to use for  $x$ , we first calculate the hydrodynamic entry length,  $x_{fd,h}$ , and the thermal entry length,  $x_{fd,t}$ , for laminar flow, which are obtained from the following equations (Equations 8.3 and 8.23 from the textbook):

$$x_{fd,h} = 0.05 Re_D D_h = 0.037 \text{ m} \quad (18)$$

$$x_{fd,t} = 0.05 Re_D D_h Pr = 0.0261 \text{ m} \quad (19)$$

For thermal boundary layer, we use Equation 6. Plugging in the parameter values, we get  $x_{fd,h} = 0.038 \text{ m}$  and  $x_{fd,t} = 0.0269 \text{ m}$ . Since  $x_{fd,h} > x_{fd,t}$  and  $x_{fd,h} < L = 0.04667 \text{ m}$ , the full length of the plate over which the air flows, we use  $x_{fd,h}$  for  $x$ . With this hydrodynamic entry length, we get  $Re_x = 1349$  and  $\delta_v = 0.005 \text{ m}$  and  $\delta_t = 0.0056 \text{ m}$ . Both boundary layer thicknesses are greater than half the gap between the plates,  $\delta_v > b/2$ , which means the boundary layer of the two adjacent plates will overlap. Therefore, it is reasonable to treat the flow as internal.

Table 6: Entry lengths and boundary layer thicknesses for laminar flow

$x_{fd,h} \text{ (m)}$	$x_{fd,t} \text{ (m)}$	$\delta_v \text{ (m)}$	$\delta_t \text{ (m)}$
0.038	0.0269	0.005	0.0056

### B.2 Fully Developed

To determine if the laminar flow is fully developed we calculate the reciprocal of Graetz number.

$$Gz^{-1} = \frac{L}{D_h Re Pr} = 0.087 > 0.05 \quad (20)$$

Since  $Gz^{-1}$  is greater than 0.05, the flow is fully developed.

### B.3 Heat Transfer Coefficient

Since the flow is internal, we can ignore free convection and only consider forced convection. The flow is laminar and fully developed, and we assume constant heat flux, so we get a Nusselt number of  $Nu_D = 8.23$  from Table 8.1 in the textbook. Then, we use Equation 9 get  $h = 47.4 \text{ W/m}^2\text{K}$ .

### B.4 Base Temperature

All other parameters remain the same as in the case of turbulent flow, including fin efficiencies. Using the same method to evaluate radiation, we use Equation 13 to get  $T_b = 31.0 \text{ }^\circ\text{C}$  for the short fin and  $T_b = 31.0 \text{ }^\circ\text{C}$  for the long fin. This gives us  $\frac{Gr}{Re_D^2} = 0.004 \ll 0.1$  for the short fin and  $\frac{Gr}{Re_D^2} = 0.0039 \ll 0.1$  for the long fin. Therefore, we have confirmed that free convection is negligible.

Table 7: Summary of calculations for turbulent and laminar flows

<i>Flow</i>	$Nu_D$	$\eta_{f,short}$	$\eta_{f,long}$	$\frac{Gr}{Re_D^2_{short}}$	$\frac{Gr}{Re_D^2_{long}}$	$Gz^{-1}$
Turbulent	10.14	0.99	0.94	0.0000175	0.0000174	N/A
Laminar	8.23			0.0040	0.0039	0.087

### **Using Fan Velocity**

For the above calculations, we used the measured velocity. However, the test bench condition was closer to 99% of the maximum value of the fan velocity given by the manufacturer ( $V=3.86\text{m/s}$ ). If we use this velocity to calculate the temperature, we get  $Re_D = 1126$ . In the case of laminar flow, we get the same values because the temperature does not depend on air velocity. In the case of turbulent flow, we get,  $Nu_D = 5.73$ ,  $h = 33.0 \text{ W/m}^2\text{K}$ , and  $T_b = 34.9 \text{ }^\circ\text{C}$  for short fins and  $T_b = 34.7 \text{ }^\circ\text{C}$  for long fins, whose average is  $T_b = 34.8 \text{ }^\circ\text{C}$ .

The calculation results are summarized in Table 7.

Table 8: Temperature and convection coefficient results

Flow	$h$ ( $W/m^2K$ )	$T_{b,short}$ ( $^{\circ}C$ )	$T_{b,long}$ ( $^{\circ}C$ )	$T_{b,avg}$ ( $^{\circ}C$ )
Turbulent ( $Re=2300$ )	58.4	29.4	29.3	<b>29.35</b>
Turbulent ( $Re=169, V=0.58$ m/s)	7.23	75.5	75.5	<b>75.5</b>
Turbulent ( $Re=1126, V=2.5$ m/s)	33.0	34.9	34.7	<b>34.8</b>
Laminar	47.4	31.0	31.0	<b>31.0</b>

*Note:  $T_b$  is equal to the temperature of the contact point between the CPU and the heat sink since the heat pipe has uniform surface temperature.*

### Conclusion for Hand Calculation

Considering all cases, the base temperature ranges from approximately 29.3  $^{\circ}C$  to 75.5  $^{\circ}C$ , which are 46.2 $^{\circ}C$  apart.  $T_b = 75.5^{\circ}C$  is unrealistically too high for turbulent flow because turbulent flow should transfer heat more efficiently than laminar flow. Moreover, the Reynolds number of 169 is much lower than the applicable range for the Nusselt correlation used for turbulent flow. Hence, the resulting temperature of 75.5 $^{\circ}C$  is more or less invalid. In conclusion, we expect the actual temperature of the base of the heat sink to be somewhere between 30 $^{\circ}C$  to 40 $^{\circ}C$ .

The temperature values obtained from SolidWorks simulation and the test bench result was near 42~44 $^{\circ}C$ . This is a bit higher than the result of hand calculation, which was 34.8 $^{\circ}C$ . There are three possible causes:

1. The actual temperature is higher most likely due to the fact that the contact resistances between the fins, heat pipes and the aluminum base were ignored in the hand calculation.
2. Also, in real situation, the presence of the heat sink would reduce the fan speed, which explains why the test bench result was higher.
3. Furthermore, the thermocouple is below the heat spreader of the CPU, so the thermocouple may be reading higher temperature than the one at the base of the heat sink due to internal conduction of the CPU.

### Test Bench Result

Table 9: Test bench parameter and results

$T_{\infty}$ ( $^{\circ}C$ )	$T_b$ ( $^{\circ}C$ )	$V_{fan}$ ( $m/s$ )
22	42	0.0056

In addition to running simulations, we ran a test using an actual AMD Phenom X4 9950 Black Edition, the CPU we used for our simulation parameters. We used the thermal paste that was supplied with the cooler.

With this system, the ambient temperature was 22°C. The CPU was fully loaded using the Prime95 stress testing program for two hours to allow the system to reach steady state. At the end of this time, the CPU temperature was 42°C according to the on-die thermocouple.



Figure 6: Test bench setup

### **SolidWorks Simulations**

In order to have an accurate and efficient flow simulation of the heat sink, multiple changes were made to the initial model. A half model analysis was tested and an element convergence was implemented for accurate and fast simulations. The experimental results from the test bench were compared with the results of the flow simulation with the same boundary conditions for additional accuracy.

### **Initial Boundary Conditions**

- Environment Pressure: 101 Kpa
- Fan RPM: 2772
- Fan Volumetric Flow Rate: 0.02560315 m<sup>3</sup>/s for full model and 0.0128 m<sup>3</sup>/s for half model
- Heat Output: 140W for full model and 70W for half model

## Materials

- Heat Pipe: Outside Surface Copper finish
- Fin and Base: Aluminum 6061

## Thermal Conductivity

- Heat Pipe: 50,000 W/(m\*K)
- Fins and Base: 170 W/(m\*K)

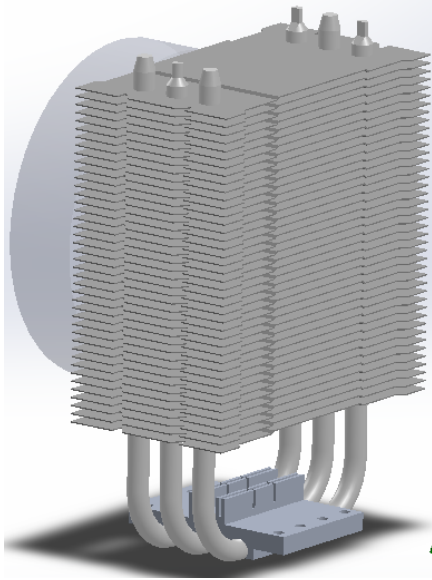


Figure 7: Initial Geometric Model

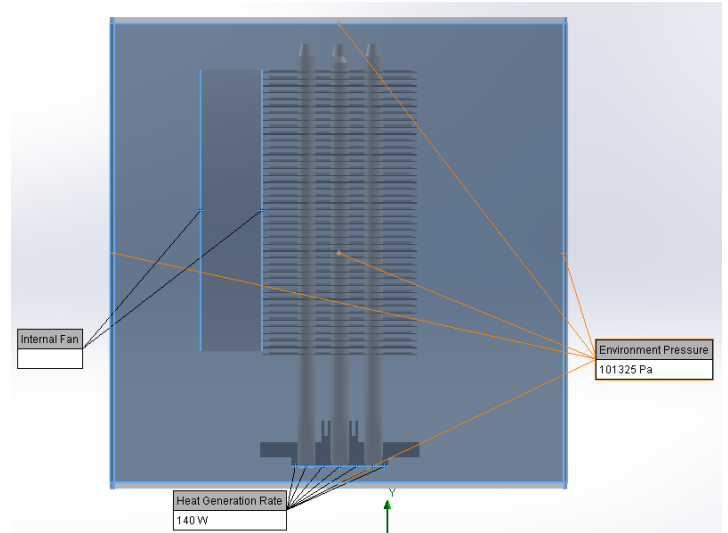


Figure 8: Initial Boundary Conditions

## Conversion from Full Model to Half Model Analysis

The initial mesh of the heat pipes and aluminum base was set to Local Mesh Solid Refinement of level 3. This was needed to initialize a comparison between a full model flow analysis and a half model flow analysis since a lower mesh brought inaccurate temperature distribution. The main goal of the flow analysis is to find the maximum temperature of heat sink at a given heat output. Since the both the heat pipe and aluminum base has direct contact with heat source, a volume goal of maximum solid temperature was set on both components.

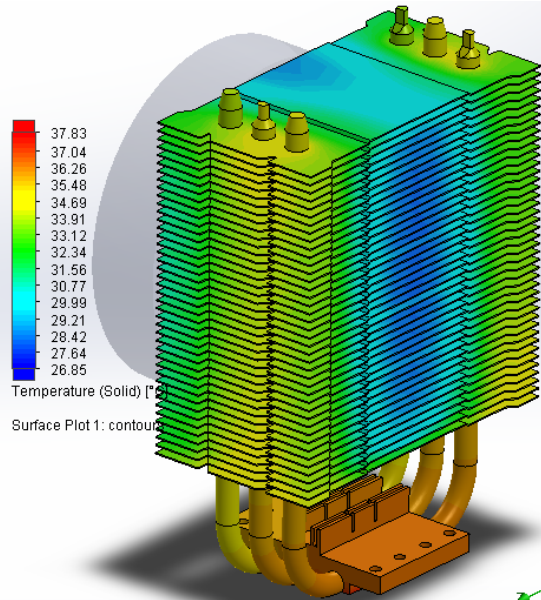


Figure 9a: Temperature distribution of full model in isometric view

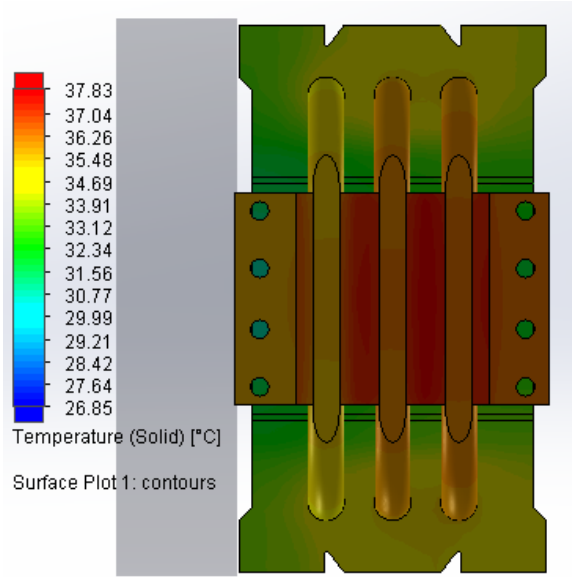


Figure 9b: Temperature distribution of full model in bottom view

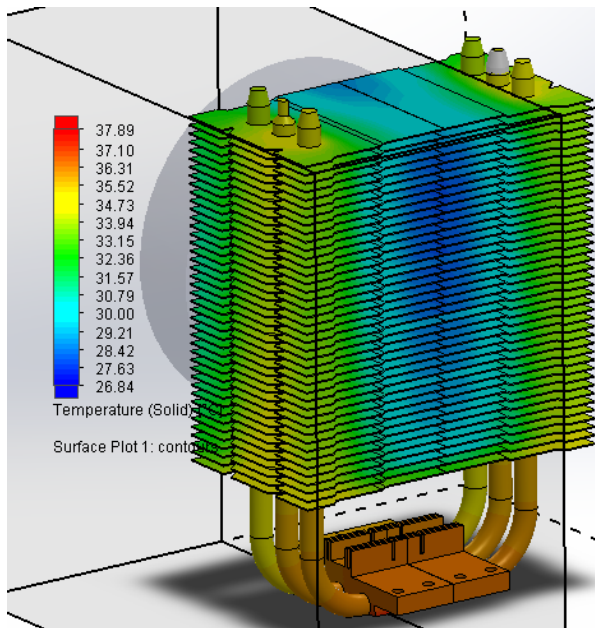


Figure 10a: Temperature distribution of half model in isometric view

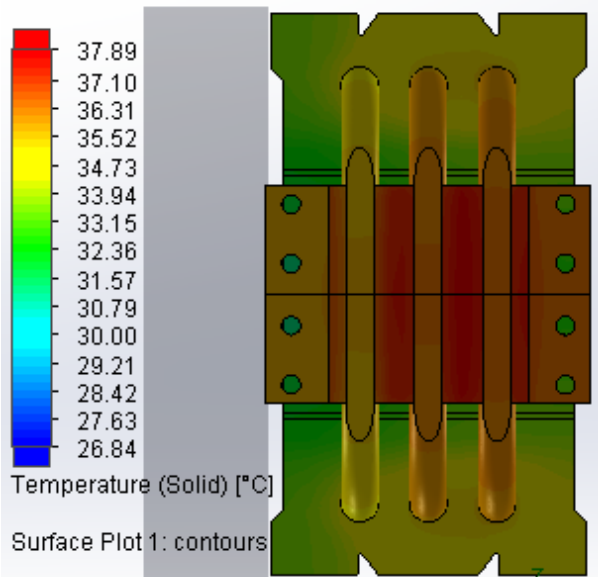


Figure 10b: Temperature distribution of half model in bottom view

Table 10: Results for Full and Half Models

Time (secs)	Total Cells	Maximum Temperature (°C)
86	59,781	37.83
47	29,933	37.89



## Conclusion

With a half model analysis, the CPU time was almost reduced in half while the maximum temperature was kept the same. The amount of cells needed for the simulations was also cut in half which explains the reduction in time. It is clear that the half model analysis is the best option for the simulation.

## Element Convergence

The number of elements were converged in order to get accurate results without losing additional CPU time. Multiple simulations were created at different solid and fluid refinement, and the maximum temperatures were examined to determined at the best refinement level that offers accuracy and minimal CPU power.

Table 11: Results for Solid Element Convergence

Solid Refinement Level	Solid Cells	Fluid Cells	Total Cells	CPU Time	Maximum Temperature (°C)
1	3,788	3,403	7,191	0:00:13	69.3098
2	11,035	12,607	23,642	0:00:26	39.1836
3	39,534	60,186	99,720	0:02:08	37.8291
4	171005	333320	504325	0:10:01	37.8869

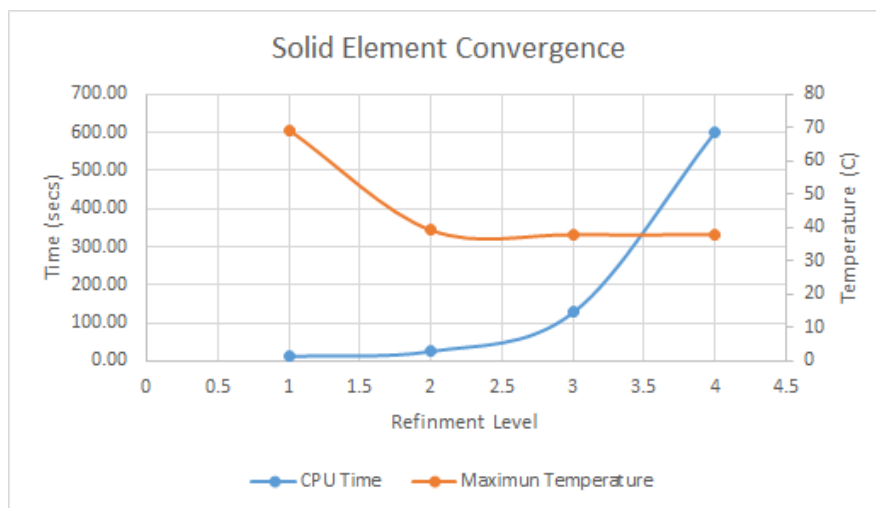


Figure 11: Solid Element Convergence Plot



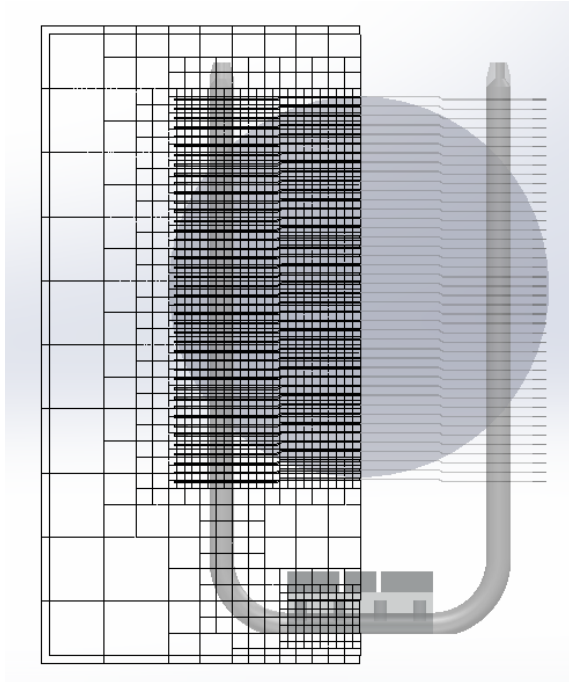


Figure 12a: Mesh of Refinement Level 3

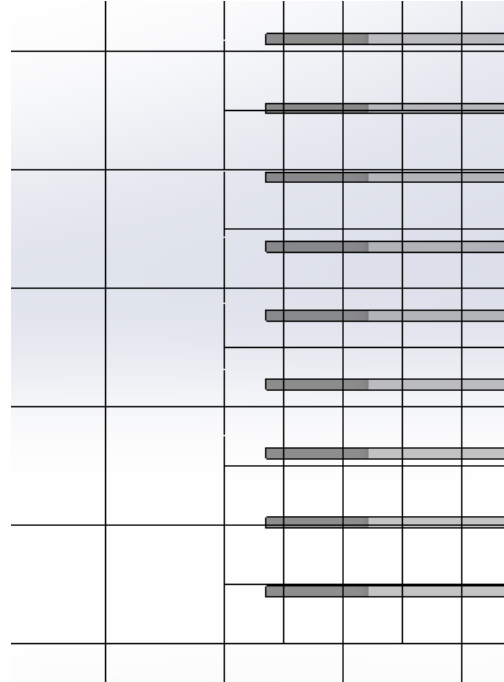


Figure 12a: Zoomed Image of Mesh of Refinement Level 3

## Conclusion

As the solid refinement increased, the number of solid elements and the CPU time increased exponentially. The maximum temperature changed had a significant change until refinement level 3. At refinement level, the CPU time increased tremendously while the temperature had minimal change. Therefore it is clear that the solid refinement level 3 is the best option.

## Refinement for Better comparison to Bench Test

### Heat Spreader

Since the CPU's thermocouple was placed on the die below the heat spreader, to increase the accuracy of the analysis and comparison to the trials, a heat spreader was modelled in the simulation. A thermal paste was added to the testing, therefore in the simulation, the contact surface was set to zero contact resistance, based on our results during lab HT-11. The material of the heat spreader was set to copper. The heat source was now implemented in the middle surface of the heat spreader, where the CPU die and the heat spreader have direct contact with thermal paste and where the thermocouple is, as shown:

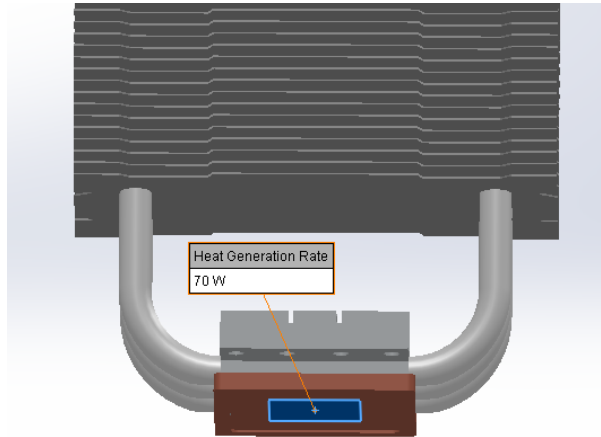


Figure 13: Model with Heat Spreader

Table 12: Element Convergence of Heat Spreader

Fluid Refinement	Total Cells	CPU Time (sec)	Max Temp of Model (°C)
0	99,981	129	41.12
2	99,981	130	41.12
4	105,294	136	41.01

Table 13: Maximum Temperature Comparison with and without Heat Spreader

	CPU Time (sec)	Max Temperature of Model (°C)
<b>No Heat Spreader</b>	128	37.83
<b>With Heat Spreader</b>	139	41.01

The maximum temperature of the model with the heat spreader is now at bottom surface of heat spreader instead of the surface base of the heat sink. The mesh refinement of the heat spreader was set to level 4. The mesh quality of the heat spreader does not matter as much since the maximum temperature and CPU time does not change as the mesh quality increases.

### Resistance

This analysis is based from Solid Refinement Level 3 with the heat spreader. Copper, ground, and air contact resistances were set on the contact surface of the heat pipe and the aluminum surfaces. Then an aluminum, ground, and air contact resistance was set on the surface of the aluminum fins and base to the heat pipe.

Table 14: Contact Resistance Comparison

Added Contact Resistance	CPU time (secs)	Maximum Temperature (°C)
No resistance	136	41.01
Added Copper Surface	137	42.03
Added Aluminum Surface	142	43.94

### Conclusion

The contact resistance makes a huge difference on the maximum temperature, changing from 41.01°C to 43.94°C, a significant difference of 2.93°C. The CPU time increased by only six seconds, therefore it is reasonable to add contact resistances for the final model analysis.

### Heat Pipe Thermal Conductivity

During our actual testing, the thermocouple measured a temperature of 42°C. The flow simulation maximum temperature does not match this temperature because of the unknown thermal conductivity value of the heat pipe. It was assumed at first that the thermal conductivity was 50,000  $W/mK$  to conduct the half model analysis, element convergence, and analysis of contact resistances and heat spreader. In order to match the simulations results to the experimental result, many simulations were produced with different thermal conductivity to figure out at what thermal conductivity the simulation's temperature matched the testing. As stated before, the thermocouple is somewhere in the middle bottom surface of the heat spreader, unspecified location. To make an accurate comparison, the average temperature of the middle surface was compared to the experimental result.

Table 15: Heat Pipe Thermal Conductivity Result Comparison

Thermal Conductivity (W/m*k)	Average Temperature (°C)	Max Temperature (°C)
10000	49.11	49.85
20000	45.49	46.19
30000	44.26	44.95
40000	43.64	44.32
60000	43.02	43.69
80000	42.7	43.37
100000	42.52	43.18

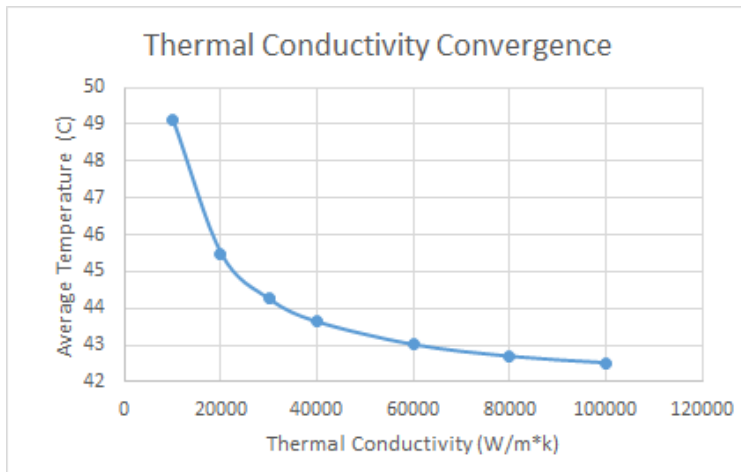


Figure 14: Heat Pipe Thermal Conductivity Result Comparison Plot

While the heat sink was not able to reach 42°C as the thermal conductivity increased, the temperature did decrease as the conductivity decreased. Below 50,000  $W/mK$ , the CPU temperature experienced the largest change, which decreased as the conductivity increased. However, the results at the higher conductivities are within the margin of error of the on-die thermocouple of the CPU, meaning that our simulation is still valid.

**Final Model Analysis**

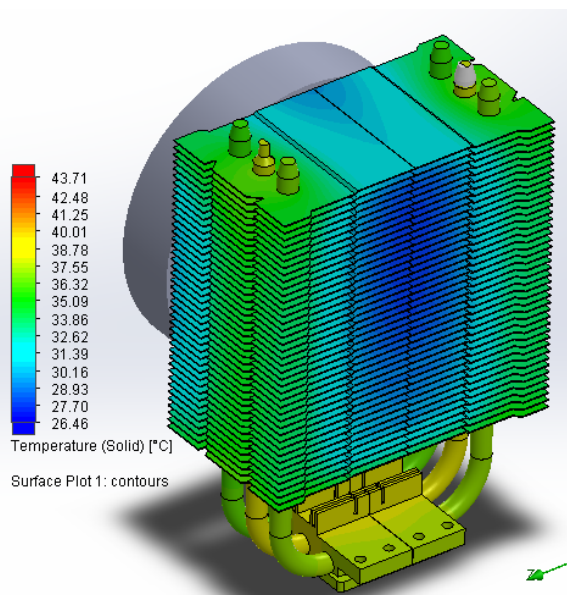


Figure 15a: Temperature distribution of final model in isometric view

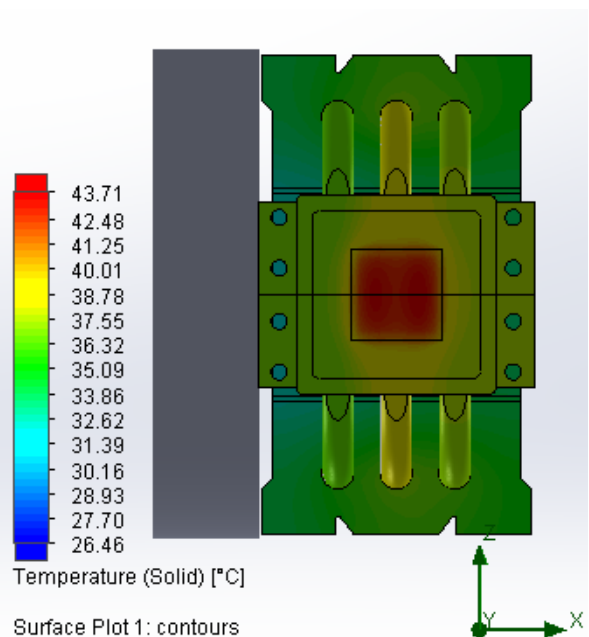


Figure 15b: Temperature distribution of final model in bottom view

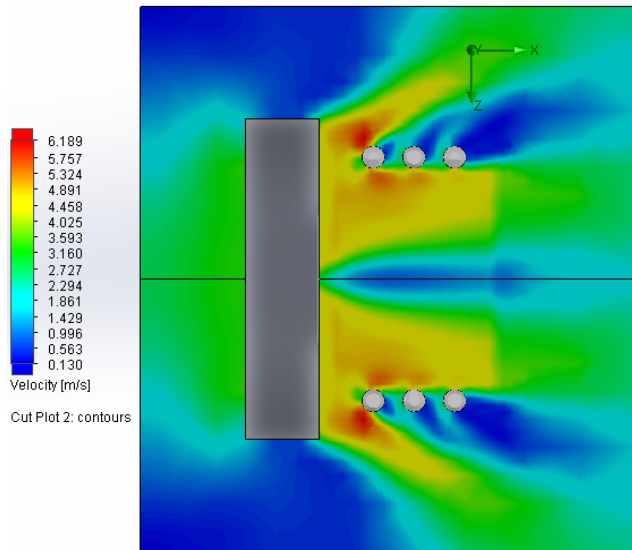


Figure 15c: Air velocity distribution in the middle of the final model

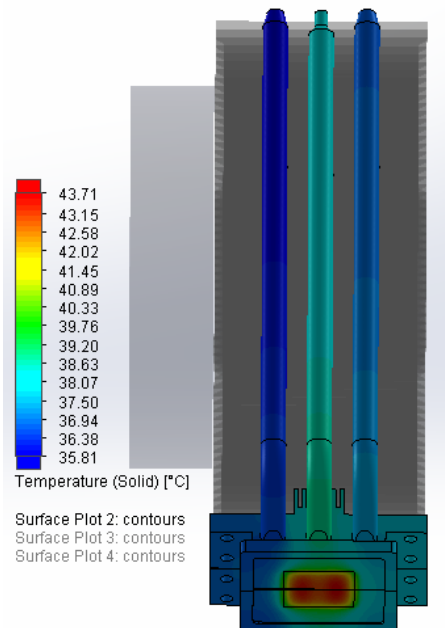


Figure 15d: Temperature distribution of heat pipe and heat spreader only

## Weakness

The model has an uncertainty of  $0.2^{\circ}\text{C}$  from the element convergence. This difference saved the simulation a huge amount of CPU time. Also the aluminum type for the fins and base is unknown, therefore the thermal conductivity might be different from the real one. However, Aluminum 6061 used in the simulation is used in most thermal situations such as this one. The biggest weakness of the simulation is the contact resistance. The exact contact resistance is unknown therefore the SolidWorks database was used. The database does not exactly match our simulation, however it is a good estimation to the real world thermal analysis.

## Strength

This simulation was compared to an experimental result therefore it can be stated that the simulation is accurate since the results are the same. For the comparison to be accurate, the heat spreader was needed in the model since the thermocouple was below the heat spreader in testing. The average temperature of the middle surface of the heat spreader was a very accurate comparison to the thermocouple measured temperature.

## Conclusion

The half model analysis allowed for the flow simulation to be faster. The element convergence added accuracy to the results while the contact resistance and the heat spreader added a more accurate comparison to the test bench results. With this in mind, the heat sink succeeded at 140W CPU since the temperature was lower than  $64^{\circ}\text{C}$ , the maximum CPU temperature allowed.

## Possible System Improvements

Our heat sink can potentially be improved with a number of physical changes. The improvements will be with respect to two different purposes:

1. *Lowering the overall manufacturing cost of the heat sink.* Since the system already achieves a temperature below the maximum processor temperature limit, it is rational to think of ways to cut down the cost while maintaining that requirement.
2. *Further enhancing the system's heat transfer ability.* We will suggest possible changes that could make the heat sink dissipate the processor's heat even better than before.

### Lowering Cost

#### 1. Remove Fan

To reduce the cost of the heat sink, one possibility is to remove the fan altogether. Since the heat sink was able to achieve a processor temperature well below the required limit, we reasoned it might be able to still do it without the help of a fan.

### Results

- Average temp: 317.87°C

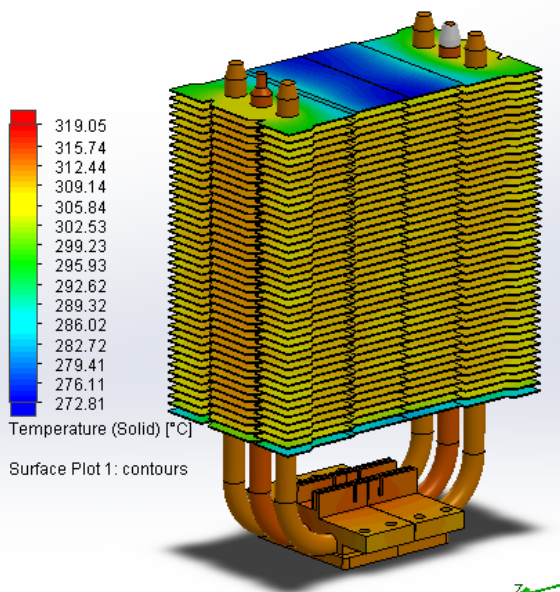


Figure 16a: Temperature distribution of model without fan in isometric view

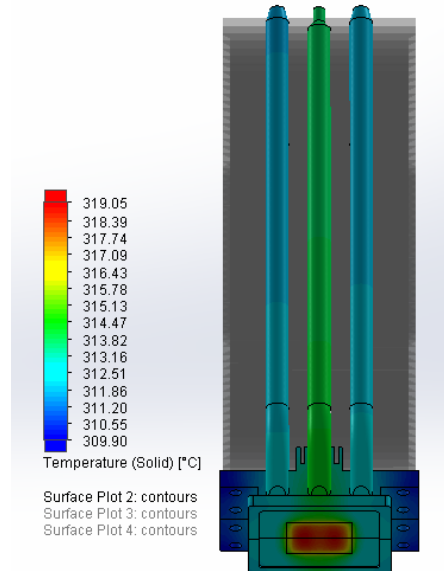


Figure 16b: Temperature distribution of heat pipe and CPU without fan

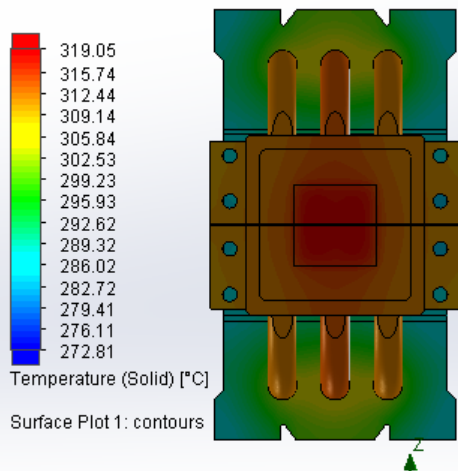


Figure 16c: Temperature distribution of model without fan in bottom view

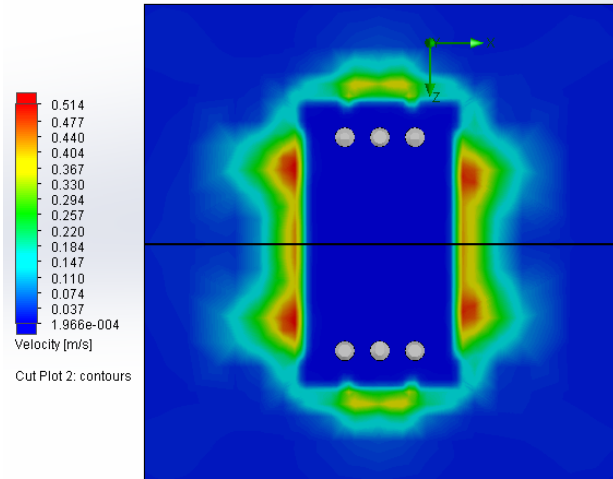


Figure 16d: Air velocity in the middle of the model without fan

## Discussion and Conclusion

The heat sink did not come close to keeping the processor below the temperature limit with a maximum temperature of nearly 318°C. It is evident that the concept of designing a heat sink small enough to fit within a desktop tower cannot be done without the help of forced convection. Without the fan, the heat tends to remain within the heat sink rather than be pushed and removed from the system due to its physical shape. This is probably what caused the average temperature to skyrocket. The conclusion of this simulation is that forced convection is absolutely essential to heat sinks. In fact, fans are probably the most efficient in terms of heat transfer versus cost.

### 2. Reducing Fin Thickness

Another way to reduce the cost of the heat sink is to lessen the material used. We reasoned that we can get away with decreasing the thickness of the fins to reduce the material used. While this may decrease the fins' ability to conduct heat, it can be tuned to stay under the maximum temperature requirement. For this simulation, we reduced the thickness of each fin from 0.35 mm to 0.25 mm, which is equivalent to 57% of the original material.

### Results

- Average: 47.17°C
- Reduce thickness from 0.35mm to 0.2mm.

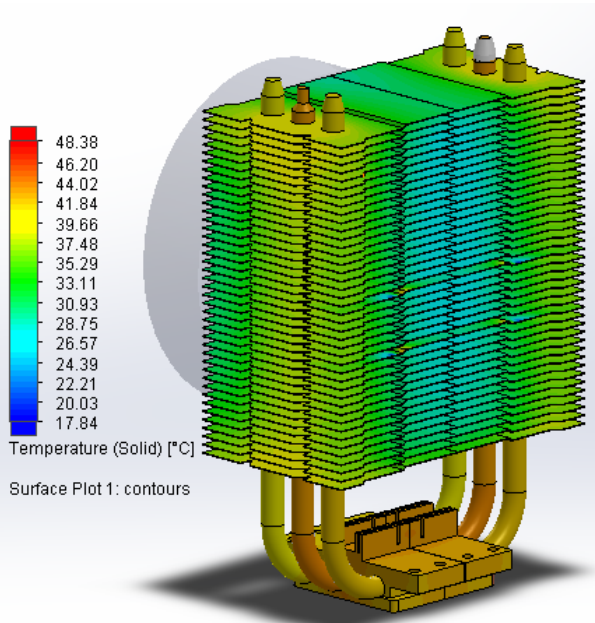


Figure 17a: Temperature distribution of model with reduced fin thickness in isometric view

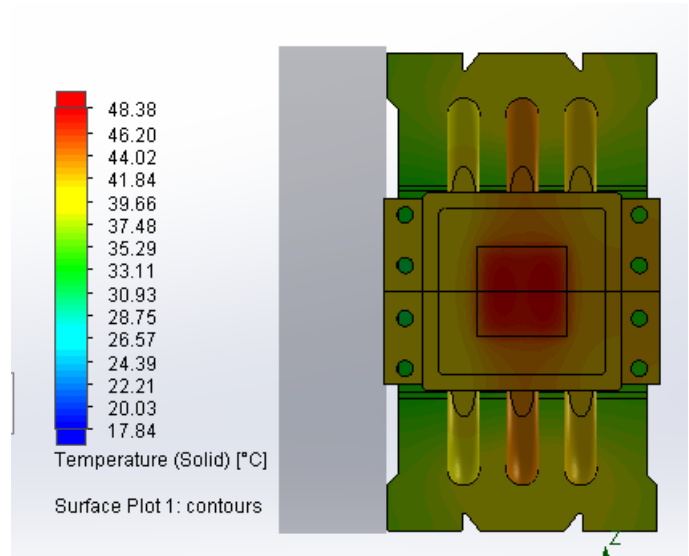


Figure 17b: Temperature distribution of model with reduced fin thickness in bottom view

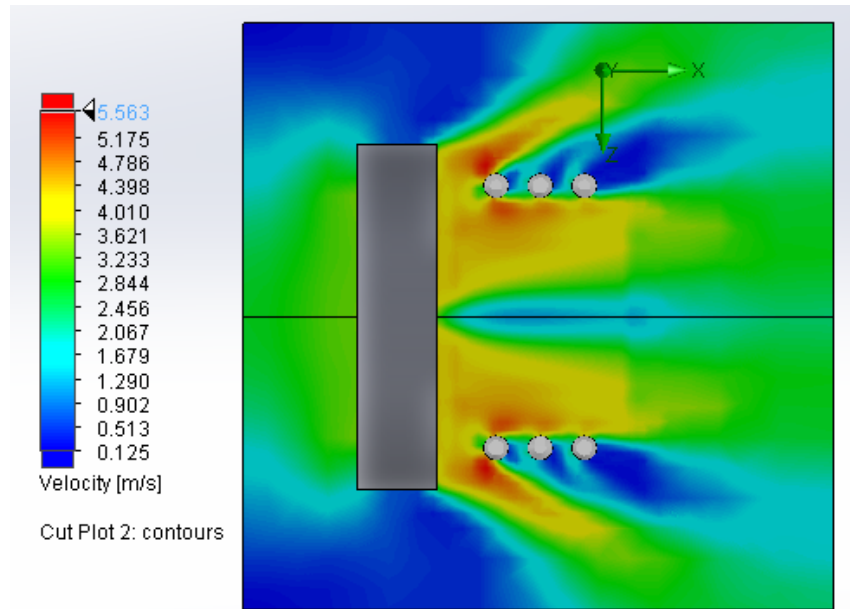


Figure 17c: Air velocity in the middle of the model with reduced fin thickness

### Discussion and Conclusion

The altered model had an average temperature of around 47°C, which is below the required maximum temperature of the processor. As expected, the temperature did increase due to its decreased ability to conduct heat due to decreased volume. However, it was still enough surface area that it was able to dissipate enough heat to achieve the requirement. With extra tuning, we



could determine a minimum thickness that the fins could manage. The conclusion of this simulation is that decreasing the thickness of the fins is an effective way to reduce cost while still meeting the maximum processor temperature requirement. However, there will be a minimum thickness since the average temperature of the system increases as the thickness decreases.

**Increasing Performance**

1. Changing Fin Material to Copper

To enhance the heat transfer ability of the heat sink, we reasoned that a fin material with a higher thermal conductivity than the current material, aluminum, would be able to do the job. Copper was the material we chose to work with since it was a common metal with among the highest thermal conductivities.

**Results**

- Average Temp: 39.19°C (3°C difference, not enough difference for higher cost)
- Changed the contact resistance from Aluminum contact to copper surface contact

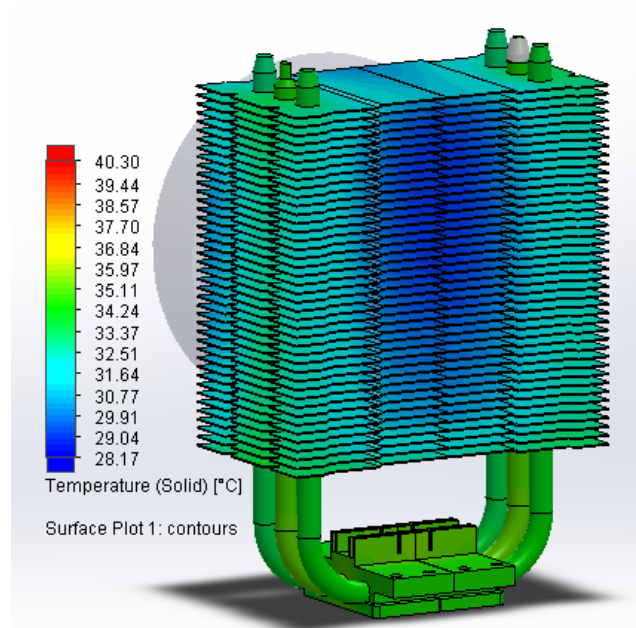


Figure 18a: Temperature distribution of model with copper fins in isometric view

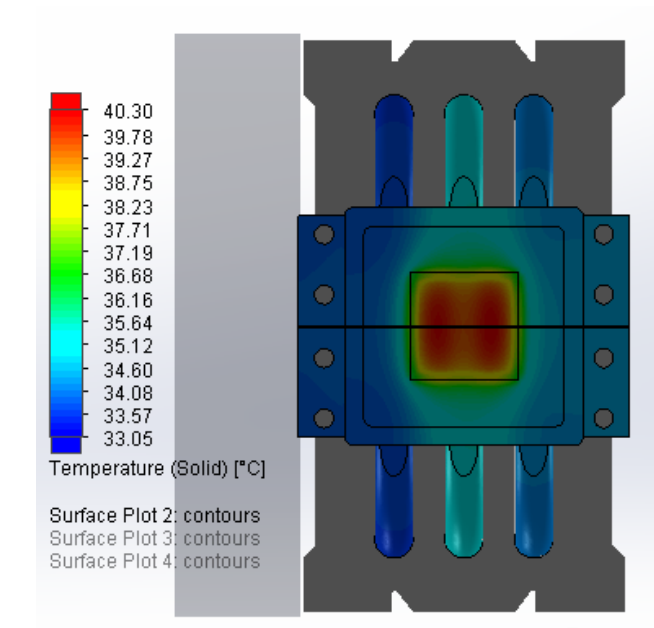


Figure 18b: Temperature distribution of model with copper fins in bottom view

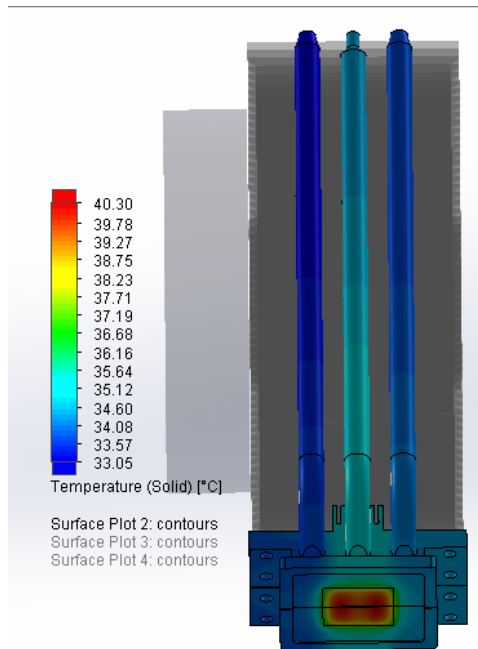


Figure 18c: Temperature distribution of heat pipe and CPU with copper fins

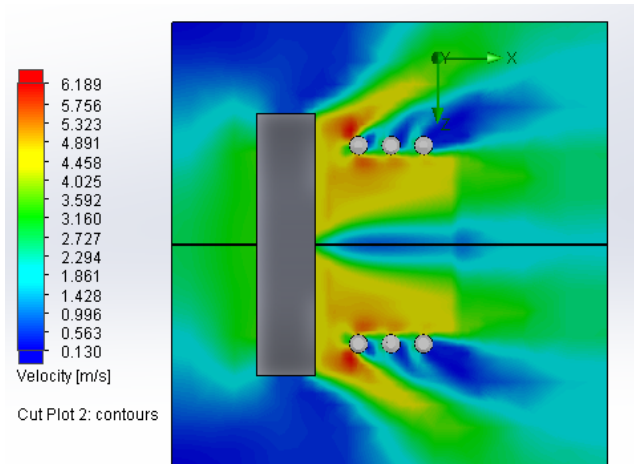


Figure 18d: Air velocity in the middle of the model with copper fins

## Discussion and Conclusion

The overall temperature of the heat sink with copper fins was about 3°C lower than the original. Changing the material to copper did enhance the system's ability to dissipate heat. This was to be expected since the material used had a better thermal conductivity than the previous material. While the temperature did go down, it didn't improve the temperature by much. If analyzed with respect to cost, the tradeoff isn't worth it. Copper is nearly three times as expensive as aluminum. The conclusion is that changing the fin material to copper cause the heat sink to perform better in terms of heat transfer. However, the cost isn't worth the change because the performance difference is too small.

### 2. Increasing Fan Speed

In theory, another way to enhance the system's performance is to increase the fan speed which would enhance forced convection. To do this, we can replace the current fan with one that is able to increase air flow. We were able to find a compatible 92mm fan called the Vantec Tornado TD9238H that had higher air flow. This fan has double the airflow rate of the original fan; around 0.56 m<sup>3</sup>/s

- AVG temp: 39.83, lower by 3°C
- RPM changed from 2800 to 4800 and volumetric flow rate from 0.0256 m<sup>3</sup>/s to 0.05616 m<sup>3</sup>/s.

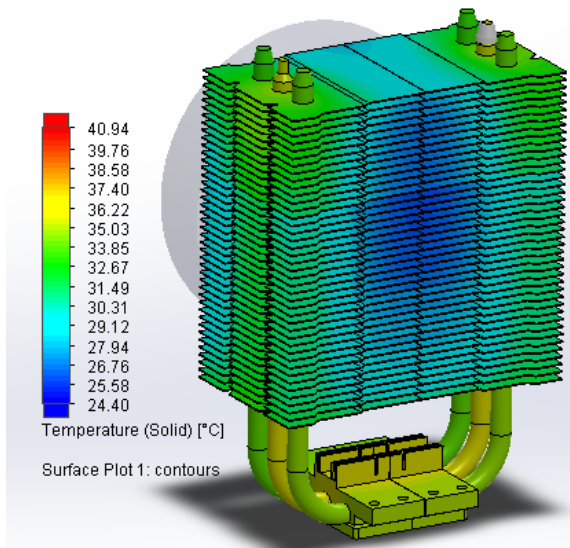


Figure 19a: Temperature distribution of model with increased fan speed in isometric view

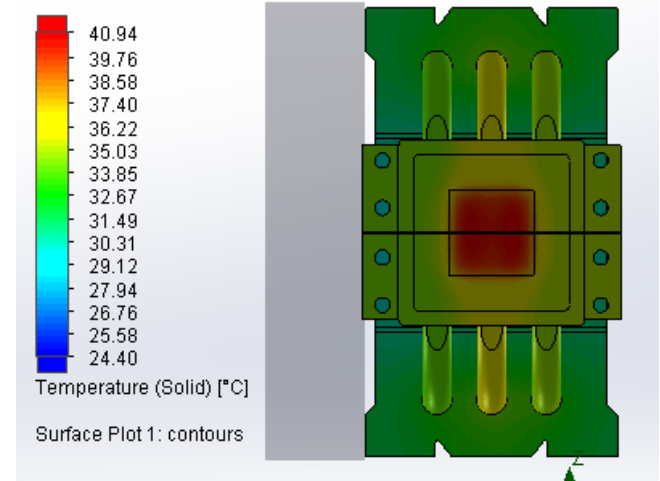


Figure 19b: Temperature distribution of model with increased fan speed in bottom view

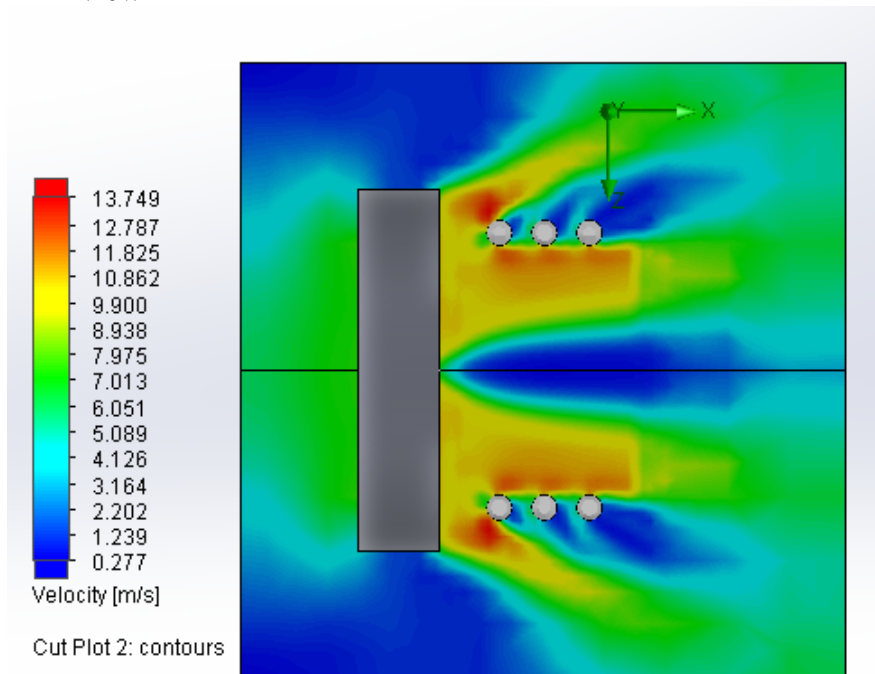


Figure 19c: Air velocity in the middle of the model with increased fan speed

## Discussion and Conclusion

The overall temperature of the heat sink with a fan about twice as much air flow was around  $3^{\circ}\text{C}$  lower than the original. Increasing air flow agreed with heat transfer theory in that increased forced convection enhances heat transfer. However, much like the last suggestion with copper,

this change is rather insignificant. This fan costs about twice as much as the original fan. The cost to performance tradeoff isn't worth it. (While the price of the fan doesn't accurately depict the actual manufacturing price, it does reflect it. Also, it's safe to assume that a fan with an increased air flow speed will be more costly.) The conclusion of this simulation is that replacing the current fan with one that can output a higher airflow rate into the heat sink will slightly enhance the system's performance. However, in terms of cost, it's not worth the change because of the insignificant change in temperature.

## References

1. "AMD Phenom X4 9950 Black Edition." *CPU-World*. N.p., 16 Feb. 2017. Web. 9 May 2017. <[http://www.cpu-world.com/CPUs/K10/AMD-Phenom%20X4%209950%20Black%20Edition%20-%20HD995ZFAJ4BGH%20\(HD995ZFAGHBOX\).html](http://www.cpu-world.com/CPUs/K10/AMD-Phenom%20X4%209950%20Black%20Edition%20-%20HD995ZFAJ4BGH%20(HD995ZFAGHBOX).html)>.
2. Bergman, Theodore L., Adrienne S. Levine, Frank P. Incropera, and David P. DeWitt. *Fundamentals of Heat and Mass Transfer*. 7th ed. N.p.: John Wiley & Sons, 2011. Print.
3. Cengel, Yunus A. and Ghajar, Afshin J. *Heat and Mass Transfer*. 5<sup>th</sup> ed. N.p.: McGrawHill Education, 2015. Print.
4. "Core i7 860." *CPU-World*. N.p., 16 Feb. 2017. Web. 9 May 2017. <[http://www.cpu-world.com/CPUs/Core\\_i7/Intel-Core%20i7-860%20BV80605001908AK%20\(BX8060517860%20-%20BXC8060517860\).html](http://www.cpu-world.com/CPUs/Core_i7/Intel-Core%20i7-860%20BV80605001908AK%20(BX8060517860%20-%20BXC8060517860).html)>.
5. "Design Considerations When Using Heat Pipes (Pt. 1)." *Celsia*. N.p., 13 June 2016. Web. 1 May 2017. <<http://celsiainc.com/blog-design-considerations-when-using-heat-pipes-pt-1/>>.
6. "FYI." *Turbulent & Laminar Flow | Heat Transfer*. Advantage Making Water Work, n.d. Web. 11 Apr. 2017. <<http://webserver.dmt.upm.es/~isidoro/tc3/Radiation%20View%20factors.pdf>>.
7. "Intel Core i7 2600k." *CPU-World*. N.p., 20 Apr. 2017. Web. 9 May 2017. <[http://www.cpu-world.com/CPUs/Core\\_i7/Intel-Core%20i7-2600K%20CM8062300833908.html](http://www.cpu-world.com/CPUs/Core_i7/Intel-Core%20i7-2600K%20CM8062300833908.html)>.
8. Martinez, Isidoro. "Radiation View Factors." *RADIATIVE VIEW FACTORS* (2017): n. pag. Web. 10 Apr. 2017. <<http://www.advantageengineering.com/fyi/156/advantageFYI156.php>>.
9. "Parallel Flow in a Straight Channel." *Objectives\_template*. NPTEL, n.d. Web. 11 Apr. 2017. <[http://nptel.ac.in/courses/112104118/lecture-25/25-3\\_parallel\\_flow.htm](http://nptel.ac.in/courses/112104118/lecture-25/25-3_parallel_flow.htm)>.
10. *The Turbulent Flat Plate Boundary Layer (Section 10-6, Çengel and Cimbala)* (n.d.): n. pag. Web. 11 Apr. 2017. <[http://www.mne.psu.edu/cimbala/me320web\\_Spring\\_2015/pdf/Flat\\_plate\\_turbulent\\_BL.pdf](http://www.mne.psu.edu/cimbala/me320web_Spring_2015/pdf/Flat_plate_turbulent_BL.pdf)>.

## Appendix A: MATLAB Code

```
%% 24-321 Thermal-Fluids Experimentation %%
% Heat Sink Project
% Lines 75,76,95 (change btw small & long fins)

clear all; close all; clc;

%% Parameters
% Properties
kc = 100000; % [W/mK] thermal conductivity of copper
ka1 = 170; % [W/mK] thermal conductivity of aluminum
ka = 25.9*10^(-3); % [W/mK] thermal conductivity of air
Pr = 0.708; % Prandtl number of air
v = 15.43*10^(-6); % 19.61*10^(-6); % [m^2/s] viscosity of air
% Universal Constants
g = 9.81; % [m/s^2] gravitational acceleration
sigma = 5.67*10^(-8); % [W/m^2K^4] Stefan-Boltzmann constant
% Dimensions
d = 0.00225; % [m] gap between two adjacent plates
L = 0.04667; % [m] full length of plate over which air flows
R = 0.003;
L1 = 0.0335;
L2 = 0.0115;
w = 0.04667;

H = 0.13793;
t = 0.00035;
N = 42; % number of fins
n = 82; % number of surfaces creating gaps
% Measurements/Calculations
T_inf = 22+273; % [K] ambient temperature
V = .58; % [m/s] air velocity *****
V = 2.5; % *****
V = 3.9*.99; % *****
qmax = 140; % [W] max heat transfer rate
% Plate dimensions
x_small = 0.09; % [m]
y_small = 0.04667; % [m]
X = x_small/d;
Y = y_small/d;

% View Factor
z = N*t;
F12 = 0.93; F36 = 1; F46 = 1; F56 = 1;
A3 = y_small*x_small; A4 = x_small*z; A5 = y_small*z; % [m^2]

%% Equations
Dh = 2*d; % [m] hydraulic diameter

%%% Turbulent %%%
Re = V*Dh/v; %2300; *****
%Re = 2300; % *****
Nu = 0.023*Re^(4/5)*Pr^0.3; % (turbulent)
x = 10*Dh; % [m] hydrodynamic entry length (turbulent)
Rex = V*x/v;
delv = 0.38*x/Rex^(1/5); % [m] velocity boundary layer thickness (turbulent)

% Laminar %%%
% Re = V*Dh/v;
% x = 0.05*Re*Dh; % [m] hydrodynamic entry length (at which laminar flow is fully developed)
% Rex = V*x/v;
% delv = 5*x/sqrt(Rex); % [m] velocity boundary layer thickness (laminar)
% Nu = 8.23;
% nf = 0.8; % (laminar)

delt = delv/Pr^(1/3); % [m] thermal boundary layer thickness
h = Nu*ka/Dh; % [W/m^2K] forced convection coefficient

Af = 2*(w*L2 - (3/2)*pi*R^2);
Lc = L2 + t/2;
At = N*Af; % + 3*(2*pi*R*(H-N*t));

P = 2*(w+t);
Ac = w*t;
```

```

m = sqrt(4*P/(kal*Ac));
nf = tanh(m*Lc)/(m*Lc);

% View Factor
term1 = log(sqrt((1+X^2)*(1+Y^2)/(1+X^2+Y^2)));
term2 = X*sqrt(1+Y^2)*atan2(X,sqrt(1+Y^2));
term3 = Y*sqrt(1+X^2)*atan2(Y,sqrt(1+X^2));
term4 = -X*atan2(X,1);
term5 = -Y*atan2(Y,1);
F12 = (2/(pi*X*Y))*(term1 + term2 + term3 + term4 + term5);

% Base Temperature
Afin = 0.090*0.04667; % total fin surface
% Asec = (L3+L1)*(L2+L4); % area of a section of fin
Asec = w*L2;
q_rad_tot = @(T) (2*sigma*(T^4 - T_inf^4)*((1+(n*(1-F12)/2))*A3*F36 + A4*F46 + A5*F56));
qconv = @(T) qmax - q_rad_tot(T);
temp = @(T) (qconv(T)*(Asec/Afin))/(h*At*(1-(N*Af/At)*(1-nf))) + T_inf - T;
Tb = fzero(temp,300);

% Natural Convection
B = 2/(Tb+T_inf); % [K^-1] coefficient of thermal expansio
Gr = g*B*(Tb-T_inf)*Dh^3/v^2; % Grashof number
ratio = Gr/Re^2;

Tb = Tb-273;

% Linear Interpolation
v1 = 26.3; %0.707; %15.87; %26.3;
v2 = 22.3; %0.720; %11.44; %22.3;
value = ((v2-v1)/(250-300))*(T_inf-300)+v1;

```